Hong Kong J Radiol. 2024;27(3):e183-91. Published 12 September 2024 | https://doi.org/10.12809/hkjr2217633

PICTORIAL ESSAY

The Different Faces of Osler-Weber-Rendu Syndrome on Radiological Imaging: A Pictorial Essay

Rajoo Ramachandran[1], Nishita Goyal[1], Sheelaa Chinnappan[1], Harini Gnanavel[1], Jagadeesan Dhanasekaran[2], Rajeswaran Rangasami[1]

[1]Department of Radiodiagnosis, Sri Ramachandra Institute of Higher Education and Research, Chennai, India
[2]Department of Intervention Radiology, Sri Ramachandra Institute of Higher Education and Research, Chennai, India

INTRODUCTION

Osler-Weber-Rendu syndrome (OWRS), also known as hereditary haemorrhagic telangiectasia (HHT), is characterised by multiple mucocutaneous telangiectasias and multiorgan arteriovenous malformations (AVMs) due to abnormal vascular remodelling traceable to a genetic defect in a binding protein for transforming growth factor. The telangiectasias and AVMs have a propensity to bleed due to their fragile nature. The multisystemic involvement of OWRS makes it imperative for clinicians and radiologists to identify the different clinical manifestations and radiological features of this syndrome. In this pictorial essay, we give an overview of the radiological features found in patients with OWRS and the role of interventional radiology in management.

RADIOLOGICAL FEATURES OF THE CASES

Three patients with a radiological diagnosis of OWRS were included (Table 1).[1-3] They underwent contrast-enhanced computed tomography (CECT) and magnetic resonance imaging (MRI) examinations followed by vascular interventions at our hospital from February 2019 to September 2020.

Computed Tomography and Magnetic Resonance Imaging Acquisition

CECT examinations of the abdomen and the pelvis were acquired using a Revolution EVO Gen 2 128-slice unit (GE HealthCare, Beijing, China). CT images were obtained with parameters of 120 kV and current in auto mode. Axial thin sections were acquired from the dome of the diaphragm to the symphysis pubis and the data were processed into multiplanar reconstruction (MPR) images with 5-mm slice thickness and three-dimensional images. The reconstruction interval was 0.625 mm. Approximately 80 mL of non-ionic contrast material (iohexol 350 mg iodine/mL; GE HealthCare, Milwaukee [WI], US) was administered with a power injector at a rate

Correspondence: *Dr N Goyal, Department of Radiodiagnosis, Sri Ramachandra Institute of Higher Education and Research, Chennai, India*
Email: drgoyalnishita@gmail.com

Submitted: 4 September 2022; Accepted: 9 May 2023.

Contributors: All authors designed the study and acquired the data. R Ramachandran, NG, SC, HG and JD analysed the data. All authors drafted the manuscript and critically revised the manuscript for important intellectual content. All authors had full access to the data, contributed to the study, approved the final version for publication, and take responsibility for its accuracy and integrity.

Conflicts of Interest: All authors have disclosed no conflicts of interest.

Funding/Support: This study received no specific grant from any funding agency in the public, commercial, or not-for-profit sectors.

Data Availability: All data generated or analysed during the present study are available from the corresponding author on reasonable request.

Ethics Approval: This study was approved by the Publication Oversight Committee of Sri Ramachandra Institute of Higher Education and Research, India [Ref No.: 11026.docx(D110578897)]. The patients were treated in accordance with the Declaration of Helsinki and informed verbal consent was obtained from the patients.

of 3.5 mL/s. Image data were acquired 18 to 20 seconds (arterial phase) and 60 seconds (portal venous phase) post contrast injection. For CT pulmonary angiography, 60 mL of non-ionic contrast was administrated intravenously at the rate of 5 mL/s followed by 30 mL of a normal saline chaser. Axial thin sections acquired from the sternal notch to the xiphisternum were used to reconstruct three-dimensional and MPR images.

For MRI of the brain, the sequences were axial T1-weighted, T2-weighted, diffusion-weighted imaging, sagittal T1-weighted, coronal fast fluid-attenuated inversion recovery, two-dimensional time-of-flight, and three-dimensional time-of-flight acquired on a Signa HDxt 1.5T scanner (GE HealthCare, Milwaukee [WI], US). The CT and MRI images were sent to a picture archiving and communication system and interpreted at workstations. Interventional procedures were performed using a biplane system (Allura Biplane FD20/20; Philips, Best, the Netherlands).

Case 1

A 43-year-old female, who had three pregnancies and three live births previously, presented with abnormal uterine bleeding for 1 month. On pelvic ultrasound, an anterior wall uterine fibroid and a right ovarian cyst was noted. A CT of the abdomen and pelvis showed a right paraovarian cyst and a heterogeneous lesion within the right lobe of the liver. CECT of the abdomen showed extensive telangiectasias[4] (Figure 1a, 1b, and Tables 2 and 3) and confluent masses[5,6] within both lobes of the liver, with the right one larger than the left one. Early opacification of the left portal vein was noted in the arterial phase, suggestive of AVMs[5] (arteriovenous shunts) [Figure 1c]. The extra- and intrahepatic arteries were dilated, with the common hepatic artery measuring around 10 mm in diameter.[5,6] On clinical examination, telangiectasias were noted in the fingertips and oral cavity of the patient.

The diagnosis of OWRS was made (Table 1[1-3]). The patient needed intervention in the liver AVMs to prevent development of portal hypertension as a complication. However, due to logistical reasons and the patient's financial difficulties, follow-up imaging was suggested.

Case 2

A 2-year-old boy presented with a sudden onset episode of generalised seizures. His father had a history of brain AVMs. On brain MRI, a bilobed extra-axial

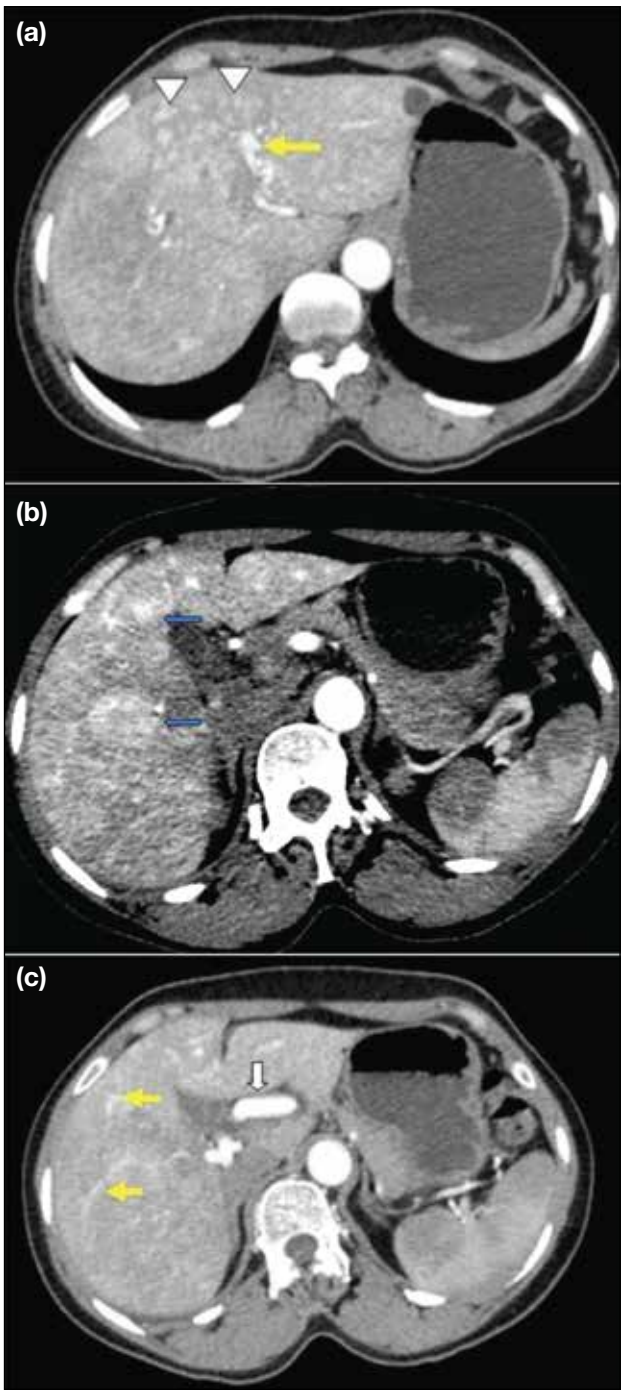

Figure 1. Case 1. Axial views of the abdomen in arterial phase at the level of the liver. (a) Multiple tiny areas of vascular puddling (arrowheads) in the hepatic parenchyma are evident, suggestive of telangiectasias. There is also early opacification of the left portal vein (yellow arrow), suggesting an arteriovenous malformation (Tables 2 and 3). (b) Medium-to-large sized vascular abnormalities representing confluent vascular masses (blue arrows) involving the right lobe of the liver are shown. (c) Multiple tortuous corkscrew-like vessels (yellow arrows) scattered in the hepatic parenchyma and the hepatic artery is dilated (white arrow), suggestive of telangiectatic vessels in Osler-Weber-Rendu syndrome.

Table 1. Curaçao clinical criteria for diagnosis of hereditary haemorrhagic telangiectasia.[1-3]

No. of features present*	Likelihood of diagnosis
≥3	Definite disease
2	Possible disease
≤2	Unlikely diagnosis

* Out of the following criteria: (1) recurrent epistaxis; (2) telangiectasias involving sites including the lips, oral cavity, nose, and fingers; (3) visceral lesions with the gastrointestinal tract, liver, pulmonary, cerebral or spinal involvement; and (4) family history of hereditary haemorrhagic telangiectasia in a first-degree relative.

lesion was seen in the right transverse temporal sulcus with blooming on gradient echo sequences and flow void on other sequences. A prominent feeder from the M4 segment of the right middle cerebral artery and a prominent vein from the superior anastomotic vein of Trolard were seen draining the lesion into the superior sagittal sinus, suggestive of AVM (Figure 2a and 2b).[1,7]

A pachygyria-polymicrogyria complex involved the right parietal lobe adjacent to the lesion (Figure 2c and 2d).[7] A large left-sided porencephalic cyst[7] communicating with the ipsilateral lateral ventricle exerted mass effect in the form of a midline shift of 7 mm to the right. There was associated left cerebral hemiatrophy (Figure 2c and 2d). The diagnosis of OWRS was made (Table 1[1-3]). In view of the high-flow AVM, embolisation was advised. Endovascular glue embolisation of the right parietal pial arteriovenous fistula was performed by administering iodixanol contrast (GE HealthCare, Milwaukee [WI], US) using a microcatheter (Excelsior XT-17; Stryker, Fremont [CA], US), microwire combination (Transcend; Meditech, Watertown [MA], US) and a HyperGlide balloon (eV3 Endovascular Inc, Irvine [CA], US) to inject 66% glue [n-butyl-2-cyanoacrylate liquid embolic system (Trufill; Cordis Neurovascular, Miami Lakes [FL], US)] as an embolisation agent mixed with ethiodised oil in various dilution ratios depending on the application to control polymerisation rate. Post-procedure angiography and brain CT were performed, which showed complete exclusion of the AVM from the circulation (Figure 2e to 2g). The patient was started on antiepileptic drugs and did not have any other seizure episode during the course in the hospital.

Case 3

A 43-year-old male presented with one episode of haemoptysis (around 10 mL of blood) and two episodes of generalised tonic-clonic seizures. Multiple scattered non-haemorrhagic lacunar infarcts were noted in the right occipital lobe and both fronto-parietal regions. Chest radiography showed multiple homogenous mass lesions in the right lower zone and left upper and lower zones (Figure 3a). Subsequent CT pulmonary angiography revealed multiple AVMs involving the anterior basal segment of the right lower lobe, the apicoposterior segment of the left upper lobe, and the lateral basal segment of the left lower lobe. Multiple tiny AVMs were identified in the right lower lobe.[8,9] The feeding artery diameter of a few of the AVMs was >3 mm[10] (Figure 3b). The diagnosis of OWRS was made (Table 1[1-3]). In view of feeding artery diameter size being >3 mm, the patient was advised to undergo curative embolisation to prevent pulmonary as well as cerebral complications. The preprocedural angiogram (Figure 3c and 3d) showed pulmonary AVMs supplied from the basal segmental arteries. Endovascular glue embolisation of the pulmonary AVMs was performed by administering iohexol contrast using a microcatheter and/or microwire and coils with 50% glue as an embolisation agent mixed with ethiodised oil in various dilution ratios. Post-embolisation angiography (Figure 3e) showed complete exclusion of the AVMs from the circulation.

DISCUSSION

Aetiologically, OWRS has been classified into different types based on the genetic mutations found in these patients. HHT type 1, found in nearly 61% of cases,[8] shows a mutation in the endoglin gene located on chromosome 9 and is found on the inner cell membrane of the endothelial cells lining the blood vessels. Patients with these mutations are generally predisposed to cerebral and pulmonary AVMs.[8] HHT type 2, found in nearly 37% of cases, shows a mutation in the activin A receptor-like type 1 (*ACVRL-1*) gene or the activin receptor-like kinase-1 (*ALK-1*) gene located on chromosome 12.[8,11] These patients have been shown to have liver AVMs.[4] Mutations in the mothers against decapentaplegic homolog 4 (*SMAD4*) gene,[9] which encodes protein for signal transmission from the transforming growth factor beta receptor, has been implicated in 2% of cases of HHT with juvenile gastrointestinal polyposis.[9] Patients having bone morphogenetic protein-9 (BMPR-9) and RSA-1 gene mutations have also shown phenotypic overlap with telangiectasia.[9]

Clinical Diagnosis, Signs, and Symptoms

The clinical diagnosis of OWRS is made using the four Curaçao clinical criteria,[1-3] namely: (1) recurrent epistaxis; (2) telangiectasias involving sites including

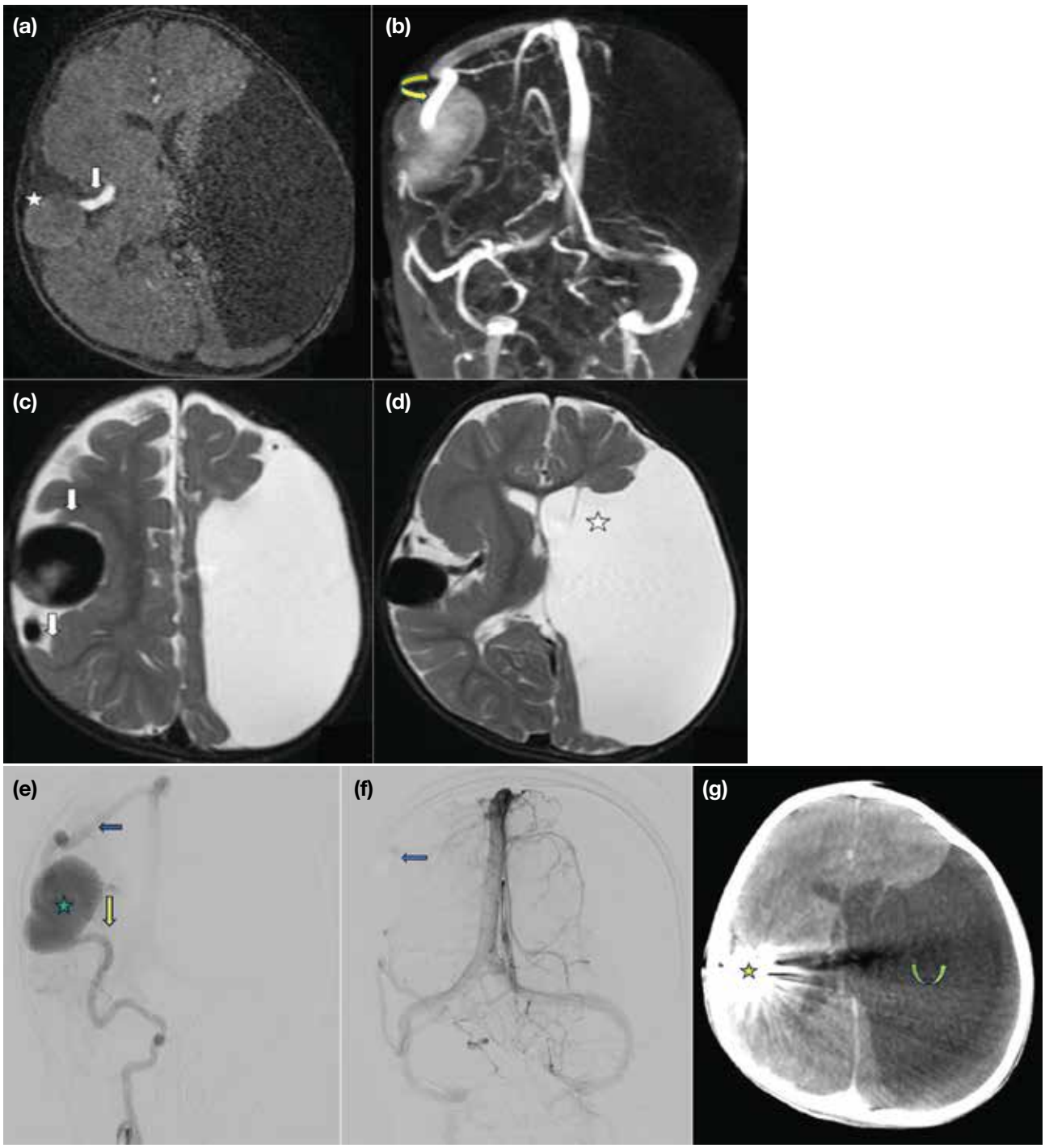

Figure 2. Case 2. (a) Axial magnetic resonance angiography showing a well-defined extra-axial lesion (star) in the right transverse temporal sulcus communicating with a prominent feeder from the M4 segment of the right middle cerebral artery (white arrow). There is associated left cerebral hemisphere atrophy. (b) Reformatted magnetic resonance venography showing a bilobed extra-axial lesion with a prominent vein representing the superior anastomotic vein of Trolard (curved yellow arrow) seen draining the lesion into the superior sagittal sinus. (c) Axial T2-weighted image (T2WI) showing a pachygyria-polymicrogyria complex (white arrows) involving the right parietal lobe adjacent to the abovementioned lesion. The lesion appears hypointense on T2WI, likely due to flow voids, suggestive of a high-flow arteriovenous fistula. (d) Axial T2WI shows an associated porencephalic cyst (star) involving the left cerebral hemisphere communicating with the frontal horn of the left lateral ventricle. (e) Preprocedural digital subtraction angiography image showing pial arteriovenous fistula involving the right fronto-parietal region fed by a right middle cerebral artery–M4 branch (yellow arrow) and draining via the vein of Trolard (blue arrow) into the superior sagittal sinus with a large venous sac (star). (f) The arteriovenous malformation (AVM) was embolised and post-procedure angiography image shows complete exclusion of the AVM from the circulation (blue arrow). (g) A non-contrast axial computed tomography of the brain shows streak artifacts secondary to post-embolisation status of the AVM (yellow star). Associated left cerebral hemisphere atrophy is noted (curved green arrow).

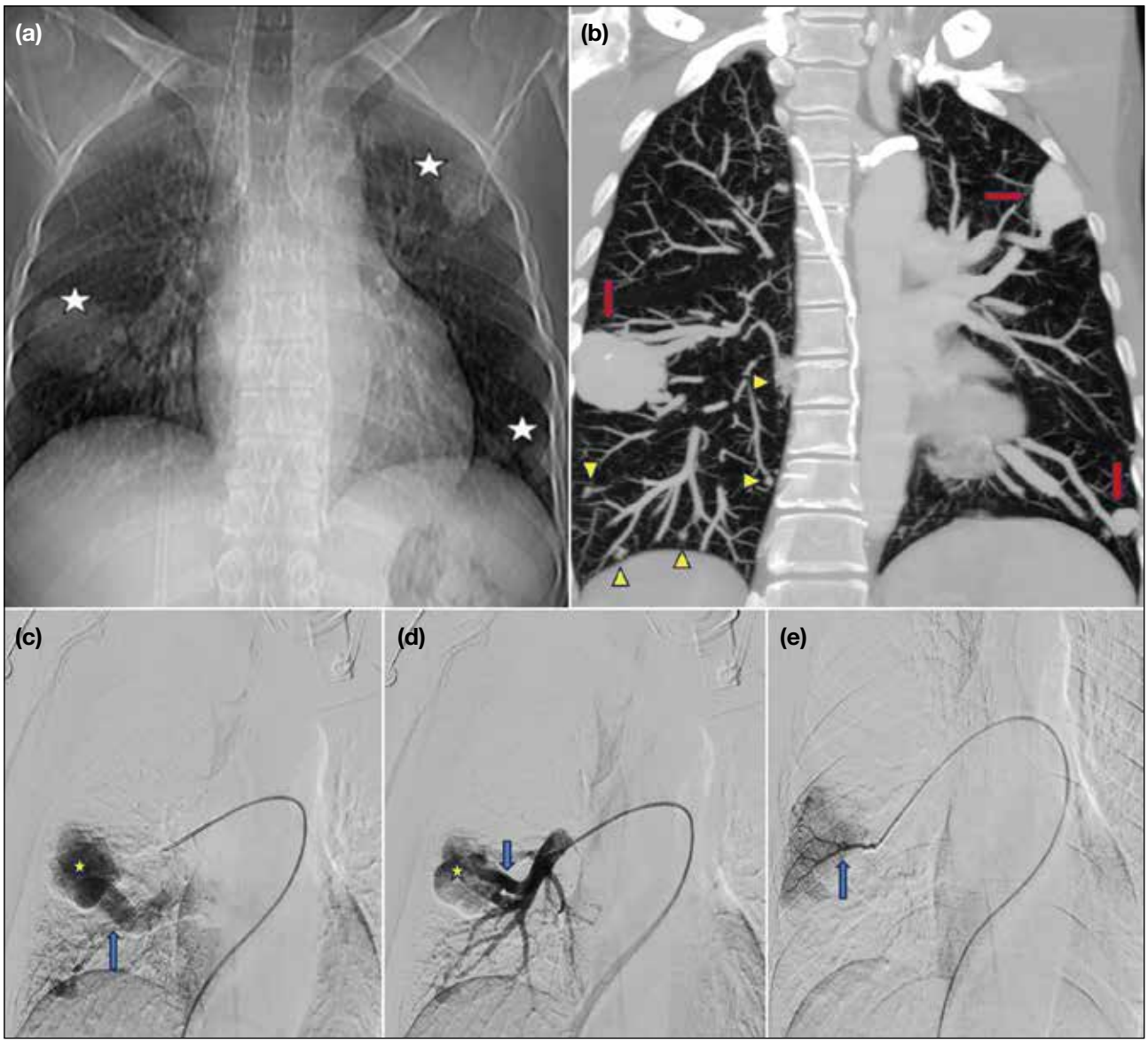

Figure 3. Case 3. (a) Chest radiograph showing multiple homogenous mass lesions (stars) seen in the right lower zone and left upper and lower zones. (b) Reformatted coronal maximum intensity projection image showing multiple arteriovenous malformations (AVMs) involving the antero-basal segment of the right lower lobe, apicoposterior segment of the left upper lobe, and the lateral basal segment of the left lobe (red arrows). Multiple tiny AVMs are seen in the right lower lobes (yellow arrowheads). (c) Pre-procedure digital subtraction angiography image of the right lung showing pulmonary AVM (star) with supply from the basal segmental arteries (blue arrow). (d) The AVM nidus (star) was progressively embolised using micro coils with 60% glue and subsequent opacification was seen. Blue arrow indicates vascular supply to the nidus from the basal segmental arteries. (e) Post-procedure angiogram shows complete exclusion of AVM from circulation (blue arrow).

the lips, oral cavity, nose, and fingers; (3) visceral lesions with the gastrointestinal tract, liver, pulmonary, cerebral or spinal involvement; and (4) family history of HHT in a first-degree relative (Table 1[1-3]).

Recurrent epistaxis is the most common symptom which can begin in childhood or adolescensce.[8] Low-pressure packing techniques can be used to manage such episodes. Telangiectasias affected individuals can present post puberty or in adulthood. It happens when capillaries fail to develop between arterioles and venules, commonly involving the face, lips, tongue, palm, and fingers (periungual and nail bed).[8] Telangiectasias can also develop in the gastrointestinal tract, presenting most commonly in the fourth decade of life with stomach and duodenum being the most common sites.[6,8] AVMs, which are direct communications between blood vessels having a

Table 2. Salient features of arteriovenous malformations within different organs with presenting signs/symptoms and treatment options.[4,8,11]

Organ involved	Liver	Pulmonary	Gastrointestinal	Brain	Spinal cord
Occurrence	~75% cases	~50% cases	30%-50% cases	~7% to 10% cases	~1% cases
Most common presentation	Generally asymptomatic	Generally asymptomatic	Gastrointestinal bleed	Asymptomatic until haemorrhagic event occurs	Back pain
Signs and symptoms	Portal hypertension, jaundice due to pressure and obstruction of bile ducts, breathlessness, fatigue due to high output cardiac failure in later stages caused by blood shunting between hepatic artery and hepatic vein	Dyspnoea, fatigue, haemoptysis, cyanosis, spontaneous haemothorax, and polycythaemia	Chronic and intermittent episodes of melena, haematemesis, and rarely haematochezia Iron deficiency anaemia may cause chest pain, breathlessness, and fatigue	Haemorrhagic events, headache, vertigo, seizure, vision abnormalities including diplopia, and hearing abnormalities Brain abscess due passage of infectious agents in paradoxical emboli from pulmonary AVMs	Functional/sensory loss in upper and lower limbs; may manifest as acute paraplegia
Screening and diagnostic imaging examinations	Doppler ultrasound screening or triple-phase helical CT	Transthoracic contrast echocardiography for screening. HRCT of the thorax for confirmation. Serpiginous masses/ nodules with ≥1 enlarged feeding artery (diameter of ≥3 mm) and a draining vein will be seen on cross-sectional imaging. Cardiomegaly and prominent pulmonary arteries are other associated imaging features	Upper and lower gastrointestinal endoscopy in adjunct to haematology screening	MRI of the brain with and without gadolinium contrast should be performed for a suspected case	MRI of the spine
Treatment strategies	First managed symptomatically For significant involvement, intravenous bevacizumab or partial resection of liver may be performed. Embolisation is not recommended due to post-embolisation necrosis risk	Transarterial pulmonary AVM vaso-occlusion with coils or transcatheter embolotherapy is the preferred treatment to prevent pulmonary or cerebral complications	Symptomatic management, endoscopic cauterisation, hormonal or antifibrinolytic therapy. Iron replacement therapy	Endovascular embolisation, stereotactic radiation, and microsurgery. Transarterial pancreatic AVM vaso-occlusion	

Abbreviations: AVM = arteriovenous malformation; CT = computed tomography; HRCT = high-resolution computed tomography; MRI = magnetic resonance imaging.

calibre greater than telangiectatic vessels, are also seen in the patients.[9,11]

Brain Involvement

Distal emboli containing blood clots or bacteria from pulmonary AVMs may result in abscess formation and ischaemic stroke (Table 2).[4,8,11]

The brain abscesses are generally multiple and recurrent, and involve the superficial layers of the cerebral lobes, most commonly occurring in the parietal lobe. A higher incidence is seen between the third and the fifth decades of life, corresponding to increased pulmonary AVMs.[4,11]

Imaging Features of Cerebral Arteriovenous Malformations

Cerebral AVMs are seen as serpiginous areas of flow void with invasion into the brain parenchyma on MRI. The feeding artery and the draining veins can be identified on different sections (Figure 2a and 2b). Some patients may have high signal intensity on T1-weighted imaging within the basal nuclei that can be a result of the metabolic disorder caused by hepatic artery-portal venous shunting. In equivocal lesions, cerebral angiography is performed, which may show high flow pial AVFs occurring due to the lack of an intervening capillary bed (Figure 2a and 2b).[1]

Table 3. Different types of hepatic shunts on radiological imaging.[5,6]

Arteriovenous shunt	Arterioportal shunt	Portal venous shunt
Most common type, occurs between hepatic artery and hepatic vein	Occurs between hepatic artery and portal vein	Rarely occurs between portal vein and hepatic vein
Visualised in the early arterial phase Telangiectasias or large vascular masses are also seen	Early enhancement of portal vein occurs in early arterial phase	Visualised in hepatic phase
Abnormal hepatic vein filling occurs during the early arterial phase and is visualised along with the intra- and extrahepatic arteries	Visualisation of paired hepatic artery and portal vein branches in early arterial phase	Dilated portal venous branch can be seen communicating with large hepatic vein through a focal hepatic mass
Rarely these shunts can cause high cardiac output heart failure and necrotising cholangitis by stealing arterial flow	Rarely these shunts can cause portal hypertension, ascites, and encephalitis	

Table 4. Important differentiating points between hereditary haemorrhagic telangiectasia and cirrhosis on radiological imaging.[5]

Hereditary haemorrhagic telangiectasia	Cirrhosis
Diffuse involvement due to underlying vascular lesions	Focal involvement due to areas of obstruction of small hepatic venules
Heterogeneous enhancement in early arterial phase with mosaic perfusion pattern showing areas of transient hepatic attenuation difference indicating arterioportal shunt	Peripheral wedge-shaped hyperattenuating lesions
Hepatic artery enlargement can be seen	Hepatic artery is of normal calibre

Cortical Development Malformation

Cortical developmental malformation is another feature which can be seen in the paediatric population. It involves two main entities: polymicrogyria and heterotopia.[7]

Patients with polymicrogyria can present with developmental delay, cognitive abnormalities, and epilepsy (about 78% of cases).[4] Epilepsy shows earlier onset in patients having higher degrees of polymicrogyria.[7] A favourable prognosis is present in patients with unilateral and localised polymicrogyria. The imaging features of polymicrogyria on MRI are smaller gyri with thin, shallow sulci separating them (Figure 2c and 2d). The cortex appears thickened, with an irregular surface and abnormal vasculature in close proximity. It is most commonly seen in the perisylvian region, followed by parietal, parietotemporal, and frontal regions.[7]

Heterotopia is an abnormal location of normal neuronal cells due to abnormal migration. The most commonly seen variant in OWRS is the periventricular nodular type. Bilateral occurrence is more common in the frontal lobes.[7]

Brain and pulmonary AVMs seem to have a higher incidence in patients with cortical developmental malformations.[7,8]

Lung Involvement

Pulmonary AVMs are the most striking features of lung involvement, seen in nearly 50% of HHT cases (Table 2).[8] The anatomical structure of AVMs can be simple, with one feeding artery and one draining vein, or complex with ≥ 2 arterial branches and draining veins.[12]

Chest radiography shows well-defined nodules within the lung (Figure 3a). Cardiomegaly and prominent pulmonary arteries can also be seen (Table 2).

Chest CT with MPR and maximum intensity projections show one or multiple serpiginous masses/nodules with ≥1 enlarged feeding artery (diameter of ≥3 mm) and draining vein (Table 2 and Figure 3b).[10,12] Contrast-enhanced magnetic resonance angiography can show all pulmonary AVMs with feeding arteries having a diameter >3 mm.[10]

The treatment of choice is transarterial pulmonary AVM vaso-occlusion with coils (Table 2).[9]

Liver Involvement

Ultrasound imaging can show an increase in common hepatic artery calibre (>7 mm) and intrahepatic hypervascularity.[6] Doppler imaging shows pulsatile portal flow in cases of arterioportal shunting and pulsatile hepatic venous flow in cases of arteriovenous shunting.[6]

Focal nodular hyperplasia and hepatic AVMs are more commonly seen in patients with *ALK-1* gene mutation. Increased sinusoidal blood flow leads to portal hypertension, pseudocirrhosis of the liver, and hepatic encephalopathy in later stages.[4,6]

Liver Telangiectasias

CECT of the abdomen with MPR and maximum intensity projections can show telangiectasias in proximity to large vessels[5] and also in the subcapsular regions. These are seen as focal hyperattenuating rounded nodular lesions in the arterial and late arterial phases, which become isodense with the hepatic parenchyma in the hepatic phase (Figure 1a, 1b, and Tables 2 and 3).[4-6] MRI shows high signal intensity on T2-weighted imaging and appears hypointense on T1-weighted imaging.

Large Confluent Masses

On CECT of the abdomen, large confluent masses within the liver (>10 mm) may be seen enhancing in enhancing arterial phase with persistent enhancement in hepatic phase.

Hereditary Haemorrhagic Telangiectasia and Cirrhosis

The differentiating features between HHT and cirrhosis on imaging for hepatic perfusion abnormalities are listed in Table 4.[5]

Pancreatic Arteriovenous Malformations

Pancreatic AVMs are the most common extrahepatic AVMs. CT imaging shows focal lesions (diameter: 5-10 mm) with increased vascularity. Arteriovenous shunting to the splenic vein or superior mesenteric vein may be noted.[5,6]

Gastrointestinal Involvement

The most common manifestation is telangiectasias, both in the small bowel (around 60%) and the stomach (around 30%). Patients with HHT have an increased incidence of small bowel polyps as compared to the general population.[6,8] Gastrointestinal haemorrhage is a common presentation, usually seen in the fourth to the fifth decades[6] (Table 2). On colonoscopy, 31% to 32% of OWRS patients show colonic AVMs associated with the HHT1 genotype having the endoglin mutation.[4] *SMAD4* mutations in OWRS patients result in juvenile polyposis, which is difficult to differentiate from the juvenile polyposis caused by BMPR1A mutations in the general population. Rarely, OWRS cases show intramural haematomas on endoscopic evaluation.[6,8,9]

Ocular Manifestations

The ocular signs and symptoms include conjunctival telangiectasias or AVMs, bloody tears, conjunctival post-haemorrhagic granulomatous lesions, and the recently described association of choriocapillaris atrophy with HHT. However, retinal involvement prevalence is only around 1%.[3,9]

Management

Embolisation of pulmonary and cerebral AVMs is important to avoid serious complications. Pulmonary AVMs having a feeding artery diameter >3 mm are ideal candidates for embolisation to decrease the risk of pulmonary haemorrhages and paradoxical emboli to the brain.[10] Patients should be advised about the side-effects related to embolotherapy for pulmonary AVMs, such as transient post-procedural chest pain and self-limiting pleurisy. Brain AVMs need treatment to prevent the occurrence of stroke and abscess. Microsurgical resection, stereotactic radiation surgery, and endovascular embolisation can be performed. Embolisation can be pre-microsurgical, pre-radiation surgery, curative, or palliative depending on the patient. Preprocedural CT angiography and antibiotic prophylaxis for the risk of bacteraemia is advised. Digital subtraction angiography is used for the procedure.[13] In our patients, since the AVMs were relatively small with few feeding pedicles and without perinidal angiogenesis, curative embolisation was performed (Table 2).

Follow-up is an important step in management of these patients. A baseline post-embolisation scan is performed at 6 months and then repeated at 12 months to ensure sac involution, followed by follow-up intervals of 2 years to detect growth of untreated pulmonary AVMs and reperfusion of treated AVMs.[14] Chest CT or contrast-enhanced MRI are used for follow-up post-coiling to look for reperfusion of occluded pulmonary AVMs.[15] The risk of reperfusion increases with larger feeding artery diameter, using less number of coils, oversized coils, or more proximal placement of the coil within the feeding artery. In such cases, it is increasingly difficult to treat these reperfused AVMs, resulting in higher recurrence rates.[15]

CONCLUSION

AVMs associated with OWRS are ticking time bombs which can result in catastrophic events such as pulmonary haemorrhages, brain abscess, stroke, chronic gastrointestinal bleeds, high-output cardiac failure, paraparesis, and, rarely, paraplegia. Since affected

individuals are generally asymptomatic, the lesions are often discovered incidentally. Radiologists must always be on the lookout for such classical findings to not only aid the diagnosis but also lower the risk of complications.

REFERENCES

1. Geibprasert S, Pongpech S, Jiarakongmun P, Shroff MM, Armstrong DC, Krings T. Radiologic assessment of brain arteriovenous malformations: what clinicians need to know. Radiographics. 2010;30:483-501.
2. Ha M, Kim YJ, Kwon KA, Hahm KB, Kim MJ, Kim DK, et al. Gastric angiodysplasia in a hereditary hemorrhagic telangiectasia type 2 patient. World J Gastroenterol. 2012;18:1840-4.
3. Rinaldi M, Buscarini E, Danesino C, Chiosi F, De Benedictis A, Porcellini A, et al. Ocular manifestations in hereditary hemorrhagic telangiectasia (Rendu-Osler-Weber disease): a case-series. Ophthalmic Genet. 2011;32:12-7.
4. Singh A, Suri V, Jain S, Varma S. Rare manifestations in a case of Osler-Weber-Rendu disease. BMJ Case Rep. 2015;2015:bcr2014207852.
5. Siddiki H, Doherty MG, Fletcher JG, Stanson AW, Vrtiska TJ, Hough DM, et al. Abdominal findings in hereditary hemorrhagic telangiectasia: pictorial essay on 2D and 3D findings with isotropic multiphase CT. Radiographics. 2008;28:171-84.
6. Jackson SB, Villano NP, Benhammou JN, Lewis M, Pisegna JR, Padua D. Gastrointestinal manifestations of hereditary hemorrhagic telangiectasia (HHT): a systematic review of the literature. Dig Dis Sci. 2017;62:2623-30.
7. Palagallo GJ, McWilliams SR, Sekarski LA, Sharma A, Goyal MS, White AJ. The prevalence of malformations of cortical development in a pediatric hereditary hemorrhagic telangiectasia population. AJNR Am J Neuroradiol. 2017;38:383-6.
8. Macri A, Wilson AM, Shafaat O, Sharma S. Osler-Weber-Rendu disease. Available from: http://www.ncbi.nlm.nih.gov/books/NBK482361/. Accessed 8 Nov 2022.
9. National Organization for Rare Disorders. Hereditary hemorrhagic telangiectasia. 2021. Available from: https://rarediseases.org/rare-diseases/hereditary-hemorrhagic-telangiectasia/. Accessed 8 Nov 2022.
10. Majumdar S, McWilliams JP. Approach to pulmonary arteriovenous malformations: a comprehensive update. J Clin Med. 2020;9:1927.
11. Maher CO, Piepgras DG, Brown RD Jr, Friedman JA, Pollock BE. Cerebrovascular manifestations in 321 cases of hereditary hemorrhagic telangiectasia. Stroke. 2001;32:877-82.
12. Lee HN, Hyun D. Pulmonary arteriovenous malformation and its vascular mimickers. Korean J Radiol. 2022;23:202-17.
13. Vollherbst DF, Chapot R, Bendszus M, Möhlenbruch MA. Glue, Onyx, Squid or PHIL? Liquid embolic agents for the embolization of cerebral arteriovenous malformations and dural arteriovenous fistulas. Clin Neuroradiol. 2022;32:25-38.
14. Hong J, Lee SY, Cha JG, Lim JK, Park J, Lee J, et al. Pulmonary arteriovenous malformation (PAVM) embolization: prediction of angiographically-confirmed recanalization according to PAVM Diameter changes on CT. CVIR Endovasc. 2021;4:16.
15. Maruno M, Kiyosue H, Hongo N, Matsumoto S, Mori H. Where is the origin of the last normal branch from feeding artery of pulmonary arteriovenous malformations? Cardiovasc Intervent Radiol. 2018;41:1849-56.